الأبحاث المنشورة(1965-1974)

فى مجال صناعة بناء وإصلاح السفن

للأستاذ الدكتور محمد عبد الفتاح شامة

Published Papers (1965-1974)

on Shipbuilding and Ship Repair

by

Prof. Dr. M. A. Shama

1- "A Design Study of a Numerically Controlled Frame Bending Machine", RINA. (UK-1965), Shama, M. A. and Miller, N. S., (90%)

2- "Plastic Bending of Short Mild Steel Beams", Bull. of the Faculty of Engineering, Alexandria University, (Egypt-1965), Shama, M. A. (100%)

3- "Behavior of Short Mild Steel Beams Bent into the Plastic Range of the Material" Bull. of the Faculty of Eng. Alexandria University, (Egypt-1967), Shama, M. A., (100%)

4- "The Impact of Application of a Numerically Controlled Plate Forming Machine on Shipyard Production" Bull of the Faculty of Engineering, Alexandria University, (Egypt-1968), Shama, M. A., 100%)

5- "Numerical Control of Plate Forming and Associated Problems", Shipbuilding and Shipping Record, Jan. (UK-1970), Shama, M. A., (100%)

6- " On the Calculation of Cold Forming Residual Stresses", Bull., Of the Faculty of Engineering, Alexandria University, Vol. XI. (Egypt-1970), Shama, M. A., (100%)

7- "Cold Forming Residual Stresses and Their Effect on the Accuracy of Post – Forming Operations", European Shipbuilding, No.2, and No. 3, Vol. 19. (Norway-1970) Shama, M. A., (100%)

8- "On the Calculation of Cold Forming Residual Stresses", Schiff und Hafen, (Germany-1974), Shama, M. A., (100%)

COLD FORMING RESIDUAL STRESSES AND THEIR EFFECT ON THE ACCURACY OF POST-FORMING OPERATIONS

By

M. A. Shama, B.Sc., Ph.D. °)

PART I.

Summary

The different sources of residual stresses are mentioned with particular reference to their adverse effect in promoting local ship failures. A simple method for calculating the magnitude and distribution of cold forming residual stresses, for any section, is given. The effect of the shape of stress-strain diagram and the section characteristics are investigated and discussed. Further, the effect of the different post-forming operations, with particular reference to punching, on the shape of the formed member is examined theoretically and experimentally.

It is concluded that cold forming residual stresses may reach values as high as the yield stress of the material. Further, the magnitude and distribution of these stresses depend mainly on the assumed shape of the stress-strain diagram, section characteristics and the degree of bend. It is also concluded that the distribution of these residual stresses should be taken into consideration, during the forming stage, in order to improve the accuracy of the post-forming operations.

Introduction

Residual stresses may result from several sources such as uneven cooling after rolling, storage, bad handling, welding (1), gas cutting ....etc. In addition to these sources, cold forming of ship plates and sections, especially when sharp curvatures are considered, introduces additional residual stresses which are probably much greater than those resulting from the other sources. These residual stresses, when superimposed, will result in a certain stress distribution, which may weaken the fatigue resistance of the material. Further, these residual stresses may have an adverse effect on the yield strength of the material as well as the buckling strength of columns (2). It is also shown in reference (3) that residual stresses have a remarkable influence on initiation and propagation of brittle fracture.

The role of residual stresses in promoting high stress concentrations or brittleness, and subsequently local ship failure, is not fully understood. Most of the research in this field appears to have been directed towards measuring the magnitude and pattern of residual stresses rather than determining their role in inducing fracture (4). Consequently, in order to assess their adverse effect residual stresses should be investigated firstly in terms of their nature and causes, magnitude and distribution, and secondly, to determine the conditions under which residual stresses may induce failure.

Apart from structural strength consideration, cold forming residual stresses can give rise to considerable distortions during the prefabrication and assembly stages, if their distribution is altered by any of the post-forming operations (welding, gas cutting .... etc.). As a result, the formed members (e.g. a frame and a plate) may not fit properly during their assembly. However, these distortions could be reduced or perhaps completely avoided, in the forming stage, by taking into acount the effect of the subsequent operations on the shape of the formed member.

The paper gives a simple method for calculating the magnitude and distribution of cold ~~calculating~~ forming residual stresses across any section using an exponential representation of the stress-strain diagram. The method is applied to fully and partially symmetrical sections, namely, rectangular and T-sections, and the results are compared with those obtained from the two alternative simple forms of stress-strain diagram, namely, ideal plastic and linear hardening. The sections considered are: a rectangular section (300 × 15 mm) and two non-standard T-sections, (300 × 15 mm, flange 50 × 20 mm) and (300 × 15 mm, flange 150 × 20 mm).

The paper also examines, theoretically and experimentally, the change in the shape of a formed

°) Lecturer in Naval Architecture Department Faculty of Engineering, Alexandria University, United Arab Republic.

member due to punching a notch at its outer edge. The tested beam (460 × 47.5 × 10 mm) was bent to a sharp curvature using the three point method on the Universal Testing Machine, and the change in shape was measured by the Universal Measuring Metroscope.

List of Notations

A_t = total sectional area
t = thickness
t_w = web thickness
t_f = flange thickness
d = depth of section
b = flange width
h = half depth of section
h_1 = distance of extreme fibres, in the web region, from the neutral axis
h_2 = distance of extreme fibres, in the flange region, from the neutral axis
X_w = distance of extreme fibres, in the web region, from the centroidal axis
X_f = distance of extreme fibres, in the flange region, from the centroidal axis
x = distance from the centroidal axis
y = distance from neutral axis
e = distance between the centroidal axis and the neutral axis
Z_e = elastic modulus of the section
Z_n = first moment of area about the fully plastic neutral axis
Z_p = plastic modulus of the section
K = shape factor
I = second moment of area about centroidal axis
I_n = second moment of area about neutral axis
M_b = bending moment
M_p = fully plastic bending moment
E = Young's modulus
ρ = radius of curvature attained by neutral axis
σ = stress
σ_y = yield stress
σ_r = residual stress
σ_b = bending stress
ε = strain
ε_y = yield strain

$\tan\alpha\alpha$ = rate of linear strain hardening.

Residual Stresses Due To Cold Bending

Residual stresses due to cold bending is in effect the result of two superimposed stress patterns. The first pattern is due to bending into the plastic range of the material and is shown in fig. (1.b). The other stress pattern results from the process of elastic recovery, or spring back, and is shown in fig. (1.a).

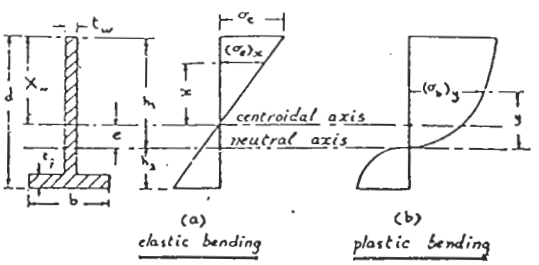

Fig. 1. Bending stress distribution.

Timoshenko (5) has given a method for calculating and measuring residual stresses. The calculations are based on the assumptions that the material is of the ideal plastic type and that the section is symmetrical about the plane of loading. Yang, Beedle and Johnston (2) have analysed. theoretically and experimentally, the residual stresses in wide flange beams, i.e. H sections, assuming that the material behaves in an ideal plastic fashion. Yen (6) has presented a method based on a linear hardening stress-strain diagram for calculating residual stresses in cold formed members. He carried out some tests to determine the distribution of these residual stresses and claimed that if the stress-strain diagram, dimensions of the cross-section and the change in curvature are known, the residual stress distribution can be calculated. However, he was mainly concerned with small curvatures and shallow sections which are not normally experienced in shipbuilding. The author, in reference (7), presented a method for calculating the distribution of residual stresses, using the linear hardening stress-strain diagram. The corresponding distribution using an ideal plastic stress-strain diagram could be obtained from the former distribution by considering zero linear rate of strain hardening. A summary of the results of these last two cases are given in Appendix (I) together with the results obtained from the exponential representation of the stress-strain diagram.

Residual Stress Distribution Using An Exponential Stress-Strain Diagram.

It is shown in reference (8) that the stress-strain diagram could be represented by the following expression:

$$\sigma = a\,\varepsilon^{1/n} \qquad \ldots (1$$

where a = constant.

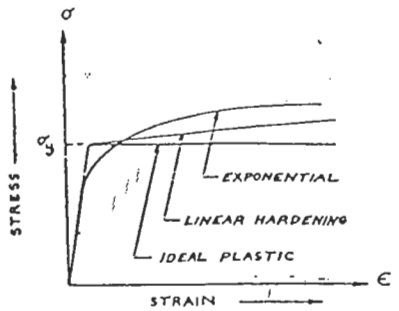

Fig. 2. Idealisation of stress strain diagam.

This representation is believed to give more realistic figures than the other two conventional forms of the stress-strain diagram, namely, ideal plastic and linear hardening, see fig. (2), when the deformations are well within the strain hardening range of the material.

The calculation of residual stresses, using this representation of stress-strain diagram, is based on the following assumptions:

1. Plane sections before bending remain plane and normal to the neutral axis, i.e.
$$\varepsilon = y/\rho \qquad \ldots\ (2)$$
2. The sections considered are symmetrical about the plane of loading and that the latter passes through the centroid of the section.
3. The unloading strain pattern is linear.
4. The bending and unloading stress distributions are uniform across the flange of the T or H sections. This assumption is valid only for deep sections with narrow flanges. However, if wide flange sections are considered, the non-uniform stress distribution across the flange should be separately investigated.
5. The change in thickness due to plastic bending is neglected.

It should be noted that the constants of equation (1) i.e. a and n are determined from the mechanical properties of shipbuilding steel, as given by the stress-strain diagram. The mean values are calculated and are as follows (9).

$a \cong 5.3$ t/sq. cm.
$n \cong 9.0$

Method of Calculation

a. Bending Stress Distribution

The bending stress distribution is obtained directly from the equation to the shape of the stress-strain diagram, as follows:

$$\sigma_b = a\left(\frac{y}{\rho}\right)^{\frac{1}{n}}$$

where a constant depending on the material properties.

b. Unloading Stress Distribution

Assuming that unloading is an elastic operation, the stress distribution is calculated according to the simple beam theory as follows:

$$(\sigma_e)_x = \frac{M.x}{I_e} \qquad \ldots\ (4)$$

where M = unloading moment = bending moment
x = distance from centroidal axis
$(\sigma_e)_x$ = the unloading stress at any depth x from the centroidal axis
I_e = second moment of area of the section about its own centroidal axis.

The unloading stress at the extreme fibres is given by:

$$\sigma_e = \frac{M.X_w}{I_e}$$

Hence: $(\sigma_e)_x = \sigma_e \frac{x}{X_w} \qquad \ldots\ (5)$

The bending moment (or unloading moment) is calculated as follows:

$$M = \int_{-h_2}^{+h_1} \sigma \cdot y \cdot dA \qquad \ldots\ (6)$$

Substituing for σ from (1), we get:

$$M = \frac{a}{(\rho)^{1/n}} \int_{-h_2}^{+h_1} y^{\frac{n+1}{n}} \cdot dA \qquad \ldots\ (7)$$

Substituting equation (7) into (4) we get:

$$(\sigma_e)_x = \left[\frac{a}{\rho^{\frac{1}{n}}} \int_{-h_2}^{+h_1} (y)^{\frac{n+1}{n}} \cdot dA\right] \cdot \frac{x}{I_e} \qquad \ldots\ (8)$$

Equation (8) represents the unloading stress distribution as function of the distance x and in terms of:

dA = elementary area at a depth y from neutral axis

h_1 and h_2 = the distances of the two extreme fibres from the neutral axis and are determined from the two equilibrium conditions:

$$\int_{o}^{AT} \sigma \cdot dA = 0 \text{ and } \int_{o}^{AT} \sigma \cdot y \cdot dA = 0 \qquad \ldots\ (9)$$

It should be noted that for fully symmetrical sections, such as a rectangular section or an I sec-

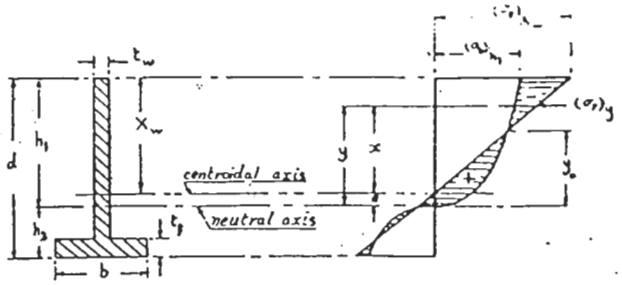

Fig. 3. Residual stress distribution.

tion, the neutral axis coincides with the centroidal axis. On the other hand, for partially symmetrical sections, such as T section, the neutral axis does not coincide with the centroidal axis.

For a T section the values of h_1 or h_2 (i.e. the position of neutral axis) are determined from the force equilibrium condition i.e.

$$\int_0^{h_1} \sigma \cdot dA = \int_0^{h_2} \sigma \cdot dA \quad \ldots\ (10)$$

Assuming that the web area is greater than the flange area, equation (10) becomes:

$$\int_0^{h_1} \sigma \cdot t_w \cdot dy = \int_0^{h_2-t_f} \sigma \cdot t_w \cdot dy + \int_{h_2-t_f}^{h_2} \sigma \cdot b \cdot dy \quad \ldots\ (11)$$

where: b = width of flange.

Substituing for σ_b from equation (3) and integrating equation (11), we obtain, after replacing h_2 by:

$$h_2 = d - h_1$$

the value of h_1, to be given by:

$$h_1 = \frac{d}{2} - \frac{t_f}{2}\left[1 - \left(\frac{b}{t_w}\right)^{\frac{n}{1+n}}\right] \quad \ldots\ (12)$$

From Fig. (3), it should be noted that:

$$y = x + e$$
$$h_1 = X_w + e$$

c. Residual Stress Distribution

The residual stress distribution is the resultant of the bending and unloading stress distributions. At any depth y from the neutral axis, it is given by:

$$(\sigma_r)_y = (\sigma_b)_y - (\sigma_e)_x \quad \ldots\ (13)$$

where: $(\sigma_r)_y$ and $(\sigma_b)_y$ are the residual and bending stress at a distance y from the neutral axis, see fig. (3).

Substituting equations (3) and (8) into equation (13), we get:

$$(\sigma_r)_y = \pm a\left(\frac{y}{\rho}\right)^{\frac{1}{n}} \mp \left[\frac{a}{\rho^{\frac{1}{n}}} \cdot \int_{-h_2}^{+h_1} y^{\frac{n+1}{n}} \cdot dA\right] \cdot \frac{x}{I_e} \quad \ldots\ (14)$$

The sign ± represents the web and flange regions respectively, when the web is subjected to tensile bending stresses, as shown in fig. (3).

Applying equation (14) for the rectangular and T sections, the residual stress distributions are given by:

i. Rectangular section:

$$(\sigma_r)_y = \pm a\left(\frac{y}{\rho}\right)^{\frac{1}{n}} \mp \frac{2\ ant}{(2n+1)\ \rho^{\frac{1}{n}}} \cdot h^{\frac{2n+1}{n}} \cdot \frac{y}{I} \quad \ldots\ (15)$$

Equation (15) is obtained from (14) by replacing:

$$dA = t\,dy$$

and $h_1 = h_2 = h$

ii. T section

The web and the flange are treated separately. For the web, replace $dA = t_w\,dy$ and for the flange, $dA = b\,dy$.

Equation (14) becomes:

$$(\sigma_r)_y = \pm a\left(\frac{y}{\rho}\right)^{\frac{1}{n}} \mp \frac{a\ n}{(2n+1)\ \rho^{\frac{1}{n}}}\left[t_w h_1^{\frac{2n+1}{n}} - b h_2^{\frac{2n+1}{n}} + (b+t_w)\ (h_2-t_f)^{\frac{2n+1}{n}}\right] \cdot \frac{y-e}{I} \quad \ldots\ (16)$$

It is noted that the residual stress distribution depends on the shape of the stress-strain diagram, section characteristics and the radius of curvature attained.

COLD FORMING RESIDUAL STRESSES AND THEIR EFFECT ON THE ACCURACY OF POST-FORMING OPERATIONS

By

M. A. Shama, B.Sc., Ph.D. °)

PART II.

Analysis Of Residual Stress Calculations.

The residual stress distribution has been calculated for three different sections, as given in Appendix (I), using the three representations of the stress-strain diagram, namely, ideal plastic, linear hardening and exponential. The results of the first two cases are based on the analysis given in reference (7) and are summarised in Appendix (I). The comparison between the three forms of stress-strain diagram is shown graphically in figs. (4, 5, 6). The numerical distribution of residual stresses across the T section (300 × 15 mm + Fl. 150 × 15 mm) is given in Table (II).

The results are summarised as follows:

1. Rectangular Section:

Fig. (4.a) shows the residual stress distribution for an ideal plastic stress-strain diagram. It is shown that the distribution is symmetrical about the neutral axis of the section. The residual stress at the neutral axis reaches the yield stress of the material. Further, the residual stress distribution is not affected by the degree of bend.

Fig. (4.b) shows the residual stress distribution for a stress-strain diagram having linear strain hardening range. It is shown that the maximum residual stress occurs either at the neutral axis or at the extreme fibres. If the elastic core is considered, when calculating residual stress distribution, the residual stress becomes zero at the neutral axis of the section..

It is also shown that the magnitude of residual stresses are lower than the corresponding values calculated according to an ideal plastic stress-strain diagram. The ratio between the corresponding values, for the two distributions, is given by:

$$1 - \frac{\tan \alpha}{E} \cong -0.9785$$

i.e. the difference is of the order of 1.2 %.

Fig. (4.c) shows the residual stress distribution for an exponential stress-strain diagram. It is shown that the residual stress at the neutral axis is zero, (because the elastic core is taken into account). Further, it is shown that the distribution depends on the degree of bend.

2. T sections

The residual stress distribution for ideal plastic stress-strain diagram, as shown in figs. (5.a) and (6.a), is not symmetrical about the neutral axis of the section. Further, the residual stress near the neutral axis, on both sides, may be as high as the yield stress of the material. It is also shown that residual stresses near the neutral axis are higher than those at the extreme fibres.

The residual stress distribution for a stress-strain diagram having linear strain hardening range as shown in figs. (5.b) and (6.b) depend in magnitude on the degree of bend. Further, the extreme fibre residual stresses may be higher than those attained near the neutral axis. It is also shown that the characteristics of the section have a great influence on the magnitude and distribution of residual stresses.

The residual stress distribution for an exponential stress-strain diagram, as shown in figs. (5.c) and (6.c), gives the magnitude of the extreme fibre residual stresses, which are shown to be less than the corresponding values obtained from the other two forms of stress-strain diagram. Further, it is shown that the magnitude and distribution of residual stresses depend on the degree of bend as well as the section characteristics.

From these results and analysis it is rather difficult to state which stress-strain diagram gives more realistic values for the distribution and magnitude of cold forming residual stresses since this conclusion could only be verified experimentally.

Effect Of Post-Forming Operations On The Shape Of A Formed Member

The subsequent operations on any formed member, such as punching, welding ... etc. will cause a redistribution of the cold forming

°) Lecturer in Naval Architecture Department Faculty of Engineering, Alexandria University, United Arab Republic.

residual stresses. As a result, the shape of the formed member will change since the section will be subjected to bending moment and normal force. This change in shape could be calculated in terms of the change in curvature at each point and also for each operation.

In the following analysis, the change in curvature due to punching, drilling or machining a notch at the outer edge of a beam will be considered.

The change in curvature could be calculated from the bending moment resulting from the unbalanced distribution of residual stresses as follows:

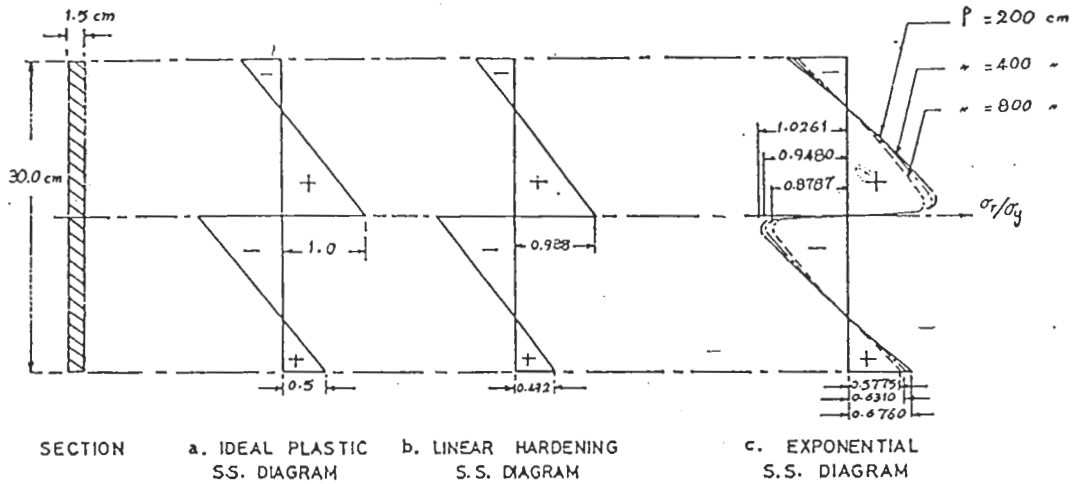

Fig. 4. Residual stress distribution for rectangular section.

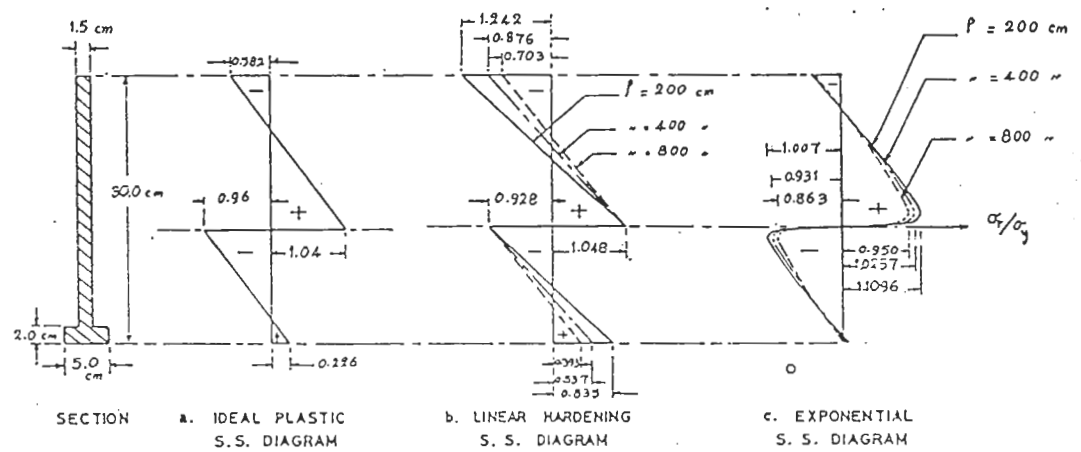

Fig. 5. Residual stress distribution for T-section No. 1.

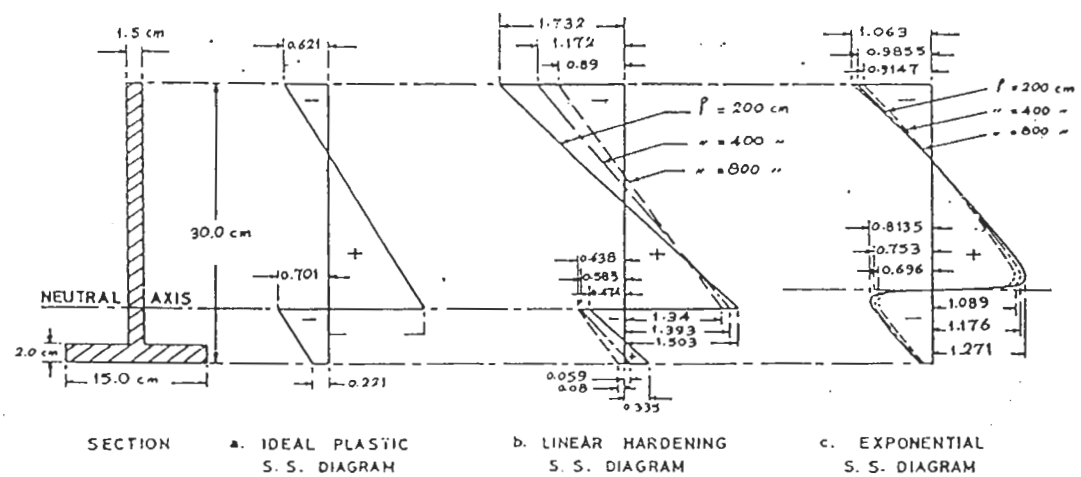

Fig. 6. Residual stress distribution for T-section No. 2.

$$\frac{1}{\rho_r} = \frac{M_r}{EI} \quad (17)$$

where: M_r = relieved bending moment, and is given by:

$$M_r = \int_{y_1}^{y_2} \sigma_r \cdot dA \cdot \bar{y} \quad (18)$$

and

$\frac{1}{\rho_r}$ = the change in the curvature of neutral axis

and I = second moment of area at the section under consideration, and is given by:

$$I = I_0 + A z^2 - (a \cdot \bar{y}^2 + i)$$

where I_0 = second moment of area about original neutral axis of section

A = total sectional area of section

z = distance between original neutral axis and final neutral axis (after notching)

a = sectional area of notch

i = second moment of notch area about its own centroidal axis

Substituting (18) into (17) we get:

$$\frac{1}{\rho_r} = \frac{1}{E} \sum_{y_1}^{y_2} \left(\frac{\sigma_r \ \Delta A \ \bar{y}}{I} \right) \quad (19)$$

where: y_1 and y_2 determine the depth of notch

$\bar{y}$ = distance of centroid of notch from new neutral axis

For a rectangular section, equation (19) could be simplified as follows:

$$\frac{1}{\rho_r} = \frac{12}{E} \cdot \sum_{y_1}^{y_2} \frac{\Delta y \cdot \bar{y}}{(2h - \Delta y)^3} \cdot \sigma_r \quad (20)$$

where: y = depth of notch = $y_2 - y_1$

$2h$ = depth of section

For the sake of accuracy, the change in curvature could be calculated by dividing the depth of notch into n division, given by:

$$\delta y = \frac{\Delta y}{n}$$

Substituting δy into equation (20), we get:

$$\frac{1}{\rho_r} = \frac{12\,\delta y}{E} \cdot \sum_{i=1}^{i=n} \frac{[h - (i-1)\frac{\delta y}{2}]}{[2h - i\,\delta y]^3} \cdot \sigma_r \quad (21)$$

where $i = 1, 2, 3 \ldots n$

$$\bar{y} = h - (i-1)\frac{\delta y}{2}$$

It should be noted that when welding or gas cutting operations are considered, additional residual stresses may be added which may increase or decrease the expected change in shape.

It should also be realised that apart from the local distortions resulting from the change in curvature, there will be a corresponding distortion at the outer end of the frame as shown in figs: (7, 8). The accumulative effect of this type of error is believed to be one of the major factors affecting misfit between prefabricated sections leading to increased assembly times and rectification costs. Therefore, in order to obviate this source of error, the expected change in curvature should be taken into account during the forming stage, however, these corrections are difficult to incorporate into the present methods of cold forming. When numerically controlled forming machines (7) are used, these corrections could be easily incorporated into the forming data.

In order to asses the degree of change in curvature, a test was carried out on a rectangular section beam.

Test Procedure And Results

The main objective of this test is to show the effect of punching a notch at the outer edge on the shape of a cold formed member.

a. Test Specimen.
A rectangular section beam (460 × 47.5 × 10.0 mm) is cut from a 10.0 mm steel plate. The length and depth of the specimen were limited by the capacity of the available bending and measuring devices.

b. Bending
The test beam is bent to a sharp curvature, as shown in figs. (9, 10) on the Universal Testing Machine, in the Material Testing Laboratory. The bending is performed using the 3-point method.

c. Measurements
Two alternative measurements for the angle θ, see fig. (10), are taken on the beam using the Universal Measuring Metroscope, Carl Zeiss, of the Metrology Laboratory, as follows:

i. By measuring the angle between the two tangent lines AB and CD, see fig. (10)

ii. By measuring the angle between the two normal lines AE and CF.

d. Notching
The beam is notched at the outer edge of the bent part for a depth of 21.5 mm. see fig. (11) in four stages as follows:

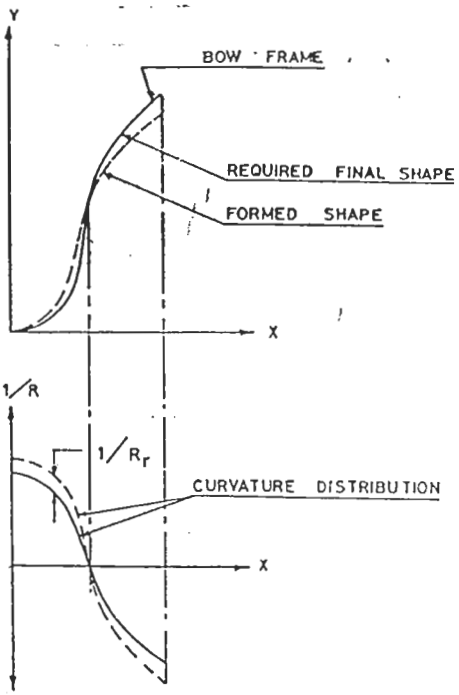

Fig. 7. Frame shape and curvature distribution.

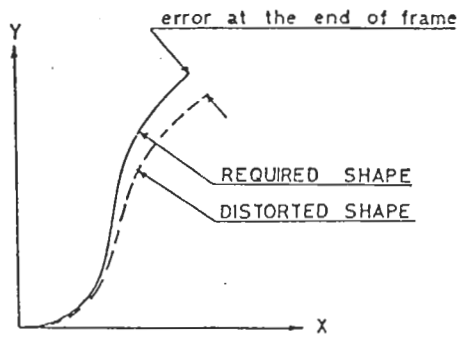

Fig. 8. Distorted frame shape.

i. first notch is rectangular and of depth 7.0 mm.
ii. second notch is triangular and of depth 7.0 mm.
iii. third notch is rectangular and of depth 7.0 mm.
iv. fourth notch is rectangular and of depth 7.5 mm.

The two alternative measurements (i) and (ii) are taken before and after punching each notch.

e. Test Results

The results of this test are given in terms of the change in the angle θ, see fig. (10) for each notch. This is because the available instruments and equipment cannot directly measure the change in curvature at the punched section.

It should be realised that a punched hole at the outer edge will not only change the curvature at the punched section, but it will also change the curvature at every section along the bent part of the beam. Consequently, the change in the angle θ does not bear any direct relation to the change in curvature at the punched section. In effect it represents the sum of the change in curvature at every section of the curved part i.e.

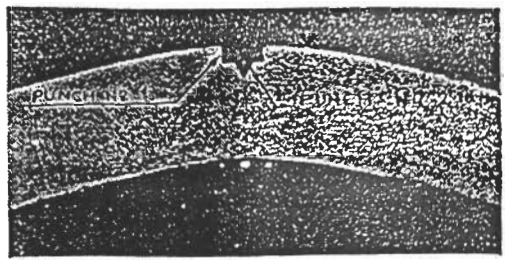

Fig. 9. Test specimen.

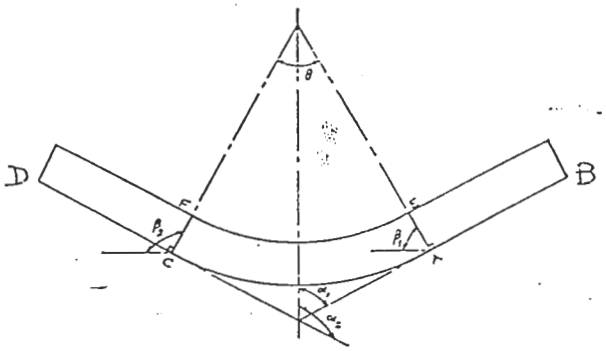

Fig. 10. Shape of bent beam.

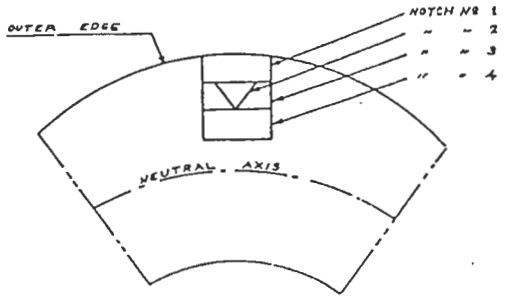

Fig. 11. Notching.

$$d\theta = \int_0^s d\left(\frac{1}{\rho}\right) dS$$

where: s = length of curved part

A summary of the test results is given in the following table:

	Notch No.			
	1	2	3	4
Depth (mm)	7.0	7.0	7.0	7.5
Change in angle θ	— 18′	— 17′	— 43′	+ 44′

The initial value of the angle θ, before notcing is = 30° 37′ 30″.

From the above results it is concluded that:

i. Punching a notch at the outer edge of a

cold formed member causes a local appreciable change in curvature.

ii. The shape, position and dimensions of the notch have a great effect on the subsequent change in shape.

iii. At a certain depth of the notch, the change in curvature changes sign. This indicates that the residual stresses change sign across the depth of section.

It should be realised that a quantitative comparison between the above results and the corresponding calculated values is only possible when the change in curvature at the punched section could be deduced from the change in the angle θ. Alternatively, this comparison is possible when the curvature at the punched section could be measured before and after punching.

CONCLUSIONS

The following are the main conclusions drawn up from the theoretical and experimental results:

1. The magnitude and distribution of residual stresses depend upon the section characteristics, shape of stress-strain diagram and the radius of curvature.
2. Cold forming residual stresses, at the extreme fibres and near the neutral axis, may reach values as high as the yield stress of the material.
3. For partially symmetrical sections, i.e. T sections, the tip residual stresses depend on the ratio of flange area to web area; the higher this ratio is, the higher the tip residual stresses will be.
4. The effect of welding, gas cutting, punching ... etc., on the shape of a cold formed member should be taken into account during the forming stage, as these operations have remarkable influence on the final shape of the member.
5. Tests should be conducted to throw some light on the actual distribution of cold forming residual stresses and to assess the accuracy of the different post-forming operations.

REFERENCES

[1]. Welding in Shipbuilding. «A Symposium by the Institute of Welding» 1961, London.

[2]. Yang, C. H., Beedle, L. S., and Johnston, B. G. «Residual Stress and the Yield Strength of Steel Beams» Progress Report No. 5., Welding Research Supplement, The Welding Journal, April, 1952, 205.

[3]. Yoshinki, M. «Review of Research Work on Large Tankers Carried out in Japan» ISSC 1961, Glasgow.

[4]. Comstock, J. B. «Review of Research Regarding Residual Stresses» I.S.S.C. 1961, Glasgow.

[5]. Timoshenko, S. P. «Strength of Materials». D. Van Nostrand Comp. Inc. 1957, Part II.

[6]. Yen, C. S. «Calculating Residual Stresses in Some Formed Parts» ASME 61-AV-38 1961.

[7]. Shama, M. A., Miller, N. «A Design Study of a Numerically Controlled Frame Bending Machine». RINA Ja. 1967, P. 95.

[8]. Shanley, F. R. «Strength of Materials». McGraw Hill Book Co., Inc. 1957.

[9]. El-Gammal, M. «Arc-welding shrinkage allowances for shipbuilding steel plates» M.Sc. Thesis Faculty of Engineering, Alexandria University, 1969.

[10]. Shama, M. A. «Plastic Bending of Short Mild Steel Beams» Faculty of Engineering Bulletin, Alexandria University, 1966.

ACKNOWLEDGEMENT

The author wishes to thank Dr. N. Damir for his help in the test.

Appendix (I)

Calculation of Residual Stress Distribution for Rectangular and Tee Sections

The sections considered are:

1. Rectangular section 300 × 15 mm.
2. Non-standard T section 300 × 15 mm + Fl. 50 × 20 mm.
3. Non-standard T section 300 × 15 mm + Fl. 150 × 20 mm.

The characteristics of these sections are given in Table (I).

For each section, the residual stress distribution is calculated using the three assumed forms of stress-strain diagram. The calculations are based on the analysis given in the text (for the exponential stress-strain diagram) and in reference (7), (for the ideal plastic and linear hardening stress-strain diagrams). The results of these calculations are given in Table (III) for both the web and flange regions. The mathematical expressions used for these calculations are summarised as follows:

1. Rectangular section

   A general solution for residual stress distribution, valid for the ideal plastic and linear hardening stress-strain diagrams is given in reference (7). The distribution of residual stresses for the ideal plastic stress-strain diagram is obtained from the general solution by replacing zero for the linear rate of strain hardening i.e. $\tan \alpha = 0$. The bending stress distribution is as given in refernce (10), i.e.:

$$\sigma_b = \pm\ (\sigma_y - \varepsilon_y \tan\alpha + \frac{y}{\rho}\tan\alpha) \quad (1)$$

The sign ± depends on the direction of bending.

The unloading elastic stress at any depth x from the centroidal axis is given by:

$$(\sigma_e)_x = \mp \frac{M}{I} \cdot x \quad (2)$$

where: $M = M_p\ (1 - \frac{\tan\alpha}{E}) + \frac{I_n \tan\alpha}{\rho}$ (3)

and is given in reference (10).

Hence: $(\sigma_e)_x = \mp [M_p(1 - \frac{\tan\alpha}{E}) + \frac{I_n \cdot \tan\alpha}{\rho}] \cdot \frac{x}{I}$ (4)

From the above expressions, the residual stress distribution is given by:

a. Linear hardening stress-strain diagram:

$$\sigma_r/\sigma_y = \pm\left(1 - \frac{\tan\alpha}{E}\right)\left(1 - \frac{k}{h} \cdot y\right) \quad (5)$$

b. Ideal plastic stress-strain diagram:

$$\frac{\sigma_r}{\sigma_y} = \pm\left(1 - \frac{k}{h} \cdot y\right) \quad (6)$$

c. Exponential stress-strain diagram:
Substituting a = 5.3 and n = 9 in equation (15) in the text, the residual stress distribution is given by:

$$\sigma_r = \pm\left[5.3\left(\frac{y}{\rho}\right)^{0.111} - 7.55\left(\frac{h}{\rho}\right)^{0.111}\frac{y}{h}\right] \quad (7)$$

2. T section
For the T section, substitute for x = y — e in expression (4).

where e = distance between centroidal and neutral axes

The residual stress distribution is given by:

a. Linear hardening stress-strain diagram:

$$\sigma_r/\sigma_y = \pm D \mp Fy \quad (8)$$

where $D = [\sigma_y - \varepsilon_y \tan\alpha] + [M_p(1 - \frac{\tan\alpha}{E}) + \frac{I_n \cdot \tan\alpha}{\rho}] \cdot \frac{e}{I}$

$$F = -\frac{\tan\alpha}{\rho} + \frac{M_p}{I}(1 - \frac{\tan\alpha}{E}) + \frac{I_n \cdot \tan\alpha}{I\rho}$$

b. Ideal plastic stress-strain diagram:

$$\sigma_r/\sigma_y = \pm\left(1 + \frac{k \cdot e}{x_w} - \frac{k}{x_w} \cdot y\right) \quad (9)$$

c. Exponential stress-strain diagram:
From equation (16) in the text, substitute for a = 5.3 and n = 9. The residual stress distribution is then simplified to:

$$\sigma_r = A \pm B y^{0.111} \pm C y \quad (10)$$

where: $A = \frac{5.03}{\rho^{0.111}}[t_w h_1^{2.111} - b h_2^{2.111} + (b + t_w)(h_2 - t_f)^{2.111}] \cdot \frac{e}{I}$

$$B = 5.3 \Big/ \rho^{0.111}$$

$$C = A/e$$

The residual stress distribution for the non-standard T section (300 × 15 mm + Fl. 150 × 20 mm) is given in Table (II) for three radii of curvature.

TABLE I

Sections Characteristics

ITEM	Rectangular section	5 CM Flange T section	15 CM Flange T section
Depth = d CM	30.0	30.0	30.0
Web thickness = t_w CM	1.5	1.5	1.5
Flange width = b CM	- - - -	5.0	15.0
Flange thickness = t_f CM	- - - -	2.0	2.0
Sectional Area = A_T CM²	45.0	52.0	72.0
Distance of extreme fibres from centroidal axis = X_w CM	15.0	16.9	20.25
Second moment of area = Ie CM⁴	3375.0	4563.7	4652.5
Sectional Modulus = Ze CM³	225.0	270.0	229.7
Plastic Modulus = Zp CM³	337.5	427.10	372.0
Shape Factor = K	1.50	1.581	1.617
Second moment of area about neutral axis = I_n CM⁴	3375.0	4573.32	5665.5
Sectional Modulus about neutral axis = Z_n CM³	225.0	254.0	236.5
Distance between centroidal axis and neutral axis = e CM	0.00	0.43	3.75

TABLE II
Residual Stress Distribution For The T Section
(300 × 15 mm, Fl. 150 × 20 mm)
Using An Exponential Stress-Strain Diagram

Location	Distance from N.A.	σ_r/σ_y		
		ρ = 800 CM	ρ = 400 CM	ρ = 200 CM
Web Region	0	+ 0.1963	+ 0.2115	+ 0.2290
	1	+ 1.0891	+ 1.1762	+ 1.2710
	2	+ 1.0539	+ 1.1379	+ 1.2300
	4	+ 0.9093	+ 0.9840	+ 1.0630
	8	+ 0.5423	+ 0.5885	+ 0.6370
	12	+ 0.1403	+ 0.1575	+ 0.1660
	16	— 0.2777	— 0.2935	— 0.3210
	21.95	— 0.9147	— 0.9855	— 1.0630
Flange Region	0	+ 0.1963	+ 0.2115	+ 0.2290
	1	— 0.6965	— 0.7532	— 0.8135
	2	— 0.6613	— 0.7149	— 0.7720
	4	— 0.5167	— 0.5610	— 0.6050
	6	— 0.3387	— 0.3715	— 0.3980
	8.05	— 0.1497	— 0.1655	— 0.1790

TABLE III

MATHEMATICAL EXPRESSIONS FOR RESIDUAL STRESS DISTRIBUTION

SECTION	ρ (cm)	STRESS STRAIN DIAGRAM			
		IDEAL PLASTIC		LINEAR HARDENING	EXPONENTIAL
		σ_r/σ_y			
Rectangular 300×15 mm	200	$\pm 1.0 \mp 0.1\,y$		$\pm 0.988 \mp 0.0988\,y$	$\pm 1.177\,y^{0.111} \mp 0.1509\,y$
	400	$\pm 1.0 \mp 0.1\,y$		$\pm 0.988 \mp 0.0988\,y$	$\pm 1.088\,y^{0.111} \mp 0.14\,y$
	800	$\pm 1.0 \mp 0.1\,y$		$\pm 0.988 \mp 0.0988\,y$	$\pm 1.008\,y^{0.111} \mp 0.1293\,y$
Tee 300×15 mm Flange 50×20 mm	200	Web	$\pm 1.04 \mp 0.0936\,y$	$\pm 1.048 \mp 0.135\,y$	$0.051 \pm 1.177\,y^{0.111} \mp 0.1184\,y$
		Fl.	$\mp 0.96 \pm 0.0936\,y$	$\mp 0.928 \pm 0.135\,y$	
	400	Web	$\pm 1.04 \mp 0.0936\,y$	$\pm 1.038 \mp 0.113\,y$	$0.0472 \pm 1.088\,y^{0.111} \mp 0.1095\,y$
		Fl.	$\mp 0.96 \pm 0.0936\,y$	$\mp 0.94 \pm 0.113\,y$	
	800	Web	$\pm 1.04 \mp 0.0936\,y$	$\pm 1.033 \mp 0.1034\,y$	$0.0436 \pm 1.008\,y^{0.111} \mp 0.1012\,y$
		Fl.	$\mp 0.96 \pm 0.0936\,y$	$\mp 0.945 \pm 0.1024\,y$	
Tee 300×15 mm Flange 150×20 mm	200	Web	$\pm 1.299 \mp 0.08\,y$	$\pm 1.503 \mp 0.135\,y$	$0.229 \pm 1.177\,y^{0.111} \mp 0.1345\,y$
		Fl.	$\mp 0.701 \pm 0.08\,y$	$\mp 0.4745 \pm 0.135\,y$	
	400	Web	$\pm 1.299 \mp 0.08\,y$	$\pm 1.393 \mp 0.107\,y$	$0.2115 \pm 1.088\,y^{0.111} \mp 0.1243$
		Fl.	$\mp 0.701 \pm 0.08\,y$	$\mp 0.583 \pm 0.107\,y$	
	800	Web	$\pm 1.299 \mp 0.08\,y$	$\pm 1.34 \mp 0.093\,y$	$0.1963 \pm 1.008\,y^{0.111} \mp 0.1152\,y$
		Fl.	$\mp 0.701 \pm 0.08\,y$	$\mp 0.638 \pm 0.093\,y$	